Structure of Subtilosin A, a Cyclic Antimicrobial Peptide from *Bacillus subtilis* with Unusual Sulfur to α-Carbon Cross-Links: Formation and Reduction of α-Thio-α-Amino Acid Derivatives[†,‡]

Karen E. Kawulka,[§] Tara Sprules,[§] Christopher M. Diaper,[§] Randy M. Whittal,[§] Ryan T. McKay,[||] Pascal Mercier,[⊥] Peter Zuber,[#] and John C. Vederas*[,§]

Department of Chemistry, Department of Biochemistry and National High Field NMR Centre (NANUC), University of Alberta, Edmonton, Alberta T6G 2G2, Canada, and Environmental and Biomolecular Systems, OGI School of Science and Engineering, Oregon Health & Science University, Beaverton, Oregon 97006 USA

Received October 31, 2003; Revised Manuscript Received January 15, 2004

ABSTRACT: The complete primary and three-dimensional solution structures of subtilosin A (**1**), a bacteriocin from *Bacillus subtilis*, were determined by multidimensional NMR studies on peptide produced using isotopically labeled [^{13}C,^{15}N]medium derived from *Anabaena* sp. grown on sodium [^{13}C]bicarbonate and [^{15}N]nitrate. Additional samples of **1** were also generated by separate incorporations of [U-^{13}C,^{15}N]-L-phenylalanine and [U-^{13}C,^{15}N]-L-threonine using otherwise unlabeled media. The results demonstrate that in addition to having a cyclized peptide backbone (amide between N and C termini), three cross-links are formed between the sulfurs of Cys13, Cys7, and Cys4 and the α-positions of Phe22, Thr28, and Phe31, respectively. The stereochemistry of all residues in **1** except for the three modified ones was confirmed to be L by complete desulfurization with nickel boride, acid hydrolysis to the constituent amino acids, and conversion of these to the corresponding pentafluoropropanamide isopropyl esters for chiral GC MS analysis. The stereochemistry at the modified residues was determined by subjecting each of the eight possible stereoisomers of **1** to eight rounds of ARIA structure calculations, starting with the same NMR peak files and assignments. The stereoisomer with the L stereochemistry at Phe22 (α-R) and D stereochemistry at Thr28 (α-S) and Phe31 (α-S) (LDD isomer) fit the NMR data, giving the lowest energy family of structures with the best rmsd. Thus, biochemical formation of the unusual thio links proceeds with net retention of configuration at Phe22, and inversion at Thr28 and Phe31. Model amino acid derivatives bearing a sulfide moiety at the α-carbon were synthesized by reaction of the corresponding α-alkoxy compounds with benzyl thiol and $SnCl_4$. Separation of their pure stereoisomers and desulfurization with nickel boride demonstrated that the reduction of such compounds proceeds with epimerization, in contrast to the previously reported retention of stereochemistry for analogous reaction of steroidal sulfides. However, desulfurization of subtilosin A to cyclic peptide **14**, which is inactive as an antimicrobial agent, occurs with inversion of stereochemistry at the α-carbons of Phe22 and Thr28 and with 4:1 retention at Phe31. This indicates that the desulfurization reaction proceeds via an N-acyl imine and that the structure of the surrounding peptide controls the geometry of reduction. Posttranslational linkage of a thiol to the α-carbon of an amino acid residue is unprecedented in ribosomally synthesized peptides or proteins, and very rare in secondary metabolites. Subtilosin A (**1**) represents a new class of bacteriocins.

Bacteriocins are potent antimicrobial peptides that are ribosomally produced by bacteria, and many are useful food preservatives (*1*, *2*). These peptides are generally cationic, range from 25 to 60 amino acids in length, and can be primarily divided into two major classes: unmodified peptides (except for disulfide bridges) and lantibiotics (*3*). The latter are extensively posttranslationally modified (*4*, *5*) by enzymatic dehydration of serine or threonine residues to give dehydroalanine or dehydrobutane moieties, which may form monosulfide lanthionine bridges through Michael attack at the β position by proximal cysteine residues. Both classes of bacteriocins are typically produced as precursors containing a leader peptide, which mediates secretion and is proteolytically removed to produce the mature, biologically active product. The detailed mechanism of action of most bacteriocins has not been established. However, in at least some cases it involves the permeabilization of the cell membrane by insertion of the peptide after interaction with a cell-surface receptor (*2*, *6*, *7*). Different types of bacteriocins vary in their modes of action. For example, the lantibiotics nisin A and mersacidin bind to lipid II (*6*, *8*−*10*), whereas certain unmodified bacteriocins appear to target a

[†] This work was supported by CanBiocin Ltd. (Edmonton), the Natural Sciences and Engineering Research Council of Canada (NSERC), the Alberta Heritage Foundation for Medical Research, and the Canada Foundation for Innovation.

[‡] The atomic coordinates of subtilosin A are available from the Protein Data Bank as entry 1PXQ.

* Corresponding author: e-mail john.vederas@ualberta.ca; tel (780) 492−5475.

[§] Department of Chemistry, University of Alberta.

[⊥] Department of Biochemistry, University of Alberta.

[||] National High Field NMR Centre (NANUC), University of Alberta.

[#] Oregon Health & Science University.

10.1021/bi0359527 CCC: $27.50
Published on Web 03/02/2004

receptor protein in the mannose phosphotransferase system (*11*, *12*). Producer organisms are insensitive to their own bacteriocins due to the production of immunity proteins which protect against membrane disruption (*13*). As bacteriocins are relatively nontoxic to eukaryotic cells, they are not only important for food preservation, but also have prospects in animal health and as human drugs (*4*, *14*). Nisin A, a lantibiotic, has been used commercially for almost 50 years as a food additive, and is now approved in over 80 countries (*15*).

Subtilosin A (**1**) is a bacteriocin produced by the Gram-positive spore forming bacterium *Bacillus subtilis* found in oriental fermented foods (*16*), and is a highly posttranslationally modified ribosomally generated peptide (*17*, *18*). The initial proposal (*17*) for the sequence and primary structure of **1** required revision following identification of its genetic locus (*18*). The mature product is formed by loss of an unusually short seven amino acid leader peptide, cyclization of the N and C termini, and further modification of Cys, Thr, and Phe residues (*18*). Subsequent studies by Marx et al. suggested that thioether bridges were present between Cys4 and Phe31, Cys7 and Thr28, and Cys13 and Phe22, but the exact nature of these cross-links was not established (*19*). In a recent preliminary report, we described the presence of novel thiol to α-carbon linkages between the modified residues in **1**, thereby identifying it as a new type of bacteriocin (*20*). In the present work, we expand our earlier results to elucidate the full primary and tertiary structure determination of **1** using both chemical and spectroscopic methods. In addition, we examine the formation and stereochemistry of nickel boride reduction of α-thio-α-amino acid derivatives in both subtilosin A (**1**) and model systems, and its use as a tool for structure elucidation of sulfur cross-linked peptides.

EXPERIMENTAL PROCEDURES

General. High-pressure liquid chromatography (HPLC) was performed on either of two instruments, a Beckman System Gold instrument equipped with a model 166 variable wavelength UV detector set at 218 nm and an Altex 210A injector with a 5-mL sample loop or a Rainin instrument equipped with a Rainin UV-1 detector set at 218 nm with 1 mL and 20 μL loops. Columns included a Waters Nova-Pak cartridge (reversed-phase Pre-Pak C18, 300-Å pore size, 15-μm particle size column), a Vydac reverse phase 208TP1010, C8, 300-Å pore size, 10-μm particle size column and a Vydac reverse phase 208TP54, C8, 300-Å pore size with a 5-μm particle size. All HPLC solvents were prepared fresh daily and filtered under vacuum before use. All aqueous solutions used milli-Q water. Labeled sodium bicarbonate and sodium nitrate were supplied by Cambridge Isotope Laboratories (Andover MA). All reactions were performed under dry Ar. All solvents were purified and distilled according to Perrin et al (*21*). Progress of reactions was monitored by TLC on commercial silica gel plates (Merck 60F-254) using UV fluorescence, ninhydrin, molybdic acid, or potassium permanganate for visualization. Flash chromatography employed silica gel 60 (Silicycle, 230−420 mesh) and was performed according to the Still procedure (*22*). Melting points were determined on a Büchi apparatus using open-end capillary tubes and are uncorrected. NMR spectra were recorded on Varian INOVA 300, 400, 500, and 800 MHz instruments. IR spectra were determined with a Nicolet Magna 750 FT-IR spectrometer. Mass spec (MS) were recorded with a Micromass ZabSpec Hybrid Sector-TOF instrument (electrospray ionization (ES)). HRMS reported values are for M+H. Optical rotations were measured on a Perkin-Elmer 241 polarimeter at 26 °C with a micro cell (100 mm; 0.9 cm^3) or a standard cell (100 mm, 8 cm^3), respectively. $[\alpha]_D$ values are given in units of 10^{-1} deg cm^2 g^{-1}. Microanalyses were completed at the University of Alberta Microanalytical Laboratory. All literature compounds had IR, ^{1}H NMR, ^{13}C NMR, and MS consistent with assigned structures.

*Growth and Purification of Subtilosin A (**1**).* Isolated colonies of *B. subtilis* strain JH642 were obtained by overnight incubation at 37 °C on DSM[1] agar plates (*23*). YT tubes (*18*) were inoculated with single colonies and grown overnight at 37 °C, with shaking at 260 rpm. YT media [1% (v/v)] was added into 7.5 mL of LB and incubated for 7 h at 37 °C. LB culture (1.5 mL) was then added to 500 mL of prewarmed NSM media (*24*) and incubated for 7 h (×2). The supernatant was extracted by adding one-quarter the volume of *n*-BuOH and shaking for 1 h (*17*), then it was poured into a separatory funnel and allowed to stand overnight. The organic layer was concentrated in vacuo and the residue resuspended in MeOH (10 mL L^{-1} of cell culture). Subtilosin A was further purified by HPLC using a Waters Nova-Pak cartridge column and a gradient from 24 to 76% CH_3CN/0.1% TFA (aq). A mixture of crude subtilosin A in MeOH/0.1% TFA (aq) 8:2 was prepared approximately 5 min before injection onto the column. Fractions containing subtilosin A, which elutes at 56% CH_3CN were combined, concentrated in vacuo, and lyophilized.

Antimicrobial Activity. Bacteriocin production was determined by the spot-on-lawn test. The indicator organism, *Listeria Monocytogenes* LI0502, was grown overnight without shaking at 30 °C in BHI broth (7.5 mL). Serial 2-fold dilutions (in LB broth) were spotted (20 μL) onto a BHI hard agar plate, allowed to dry, and overlaid with 7.5 mL of a 1% LI0502 inoculated BHI soft agar. Zones of inhibition were measured following 16 h incubation at 37 °C. Results are expressed in AU of bacteriocin (1 AU is the amount of bacteriocin required to produce visible clearing on a lawn of indicator strain).

Mass Spectroscopy. MALDI-TOF mass spectrometry employed a 1:2 mixture of approximately 1 to 10 μg/μL subtilosin A in MeOH/0.1% TFA (aq) 7:3 and a saturated solution of sinapinic acid (MeOH/0.1% TFA (aq) 1:3). The samples were analyzed on an Applied Biosystems Voyager Elite MALDI TOF system equipped with delayed extraction and an ion mirror (reflectron) for improving resolution and mass accuracy. External calibration was performed with a mixture of bovine insulin chain B (oxidized form) and bovine insulin.

Preparation of Labeled Peptone. Labeled peptone media (^{13}C,^{15}N) was produced by fermentation of *Anabaena* sp.

[1] Abbreviations: NOE, nuclear Overhauser effect; TBDMSCl, *tert*-butyldimethylsilyl chloride; DMF, *N*,*N*-dimethylformamide; DSM, Difco sporulation medium; GC, MS gas chromatography mass spectrometry; PFPA, pentafluoropropanoyl anhydride; SAM, *S*-adenosoylmethionine; SubA, subtilosin A; MoaA, molybdenum cofactor biosynthesis protein A; NifB, nitrogen fixation gene B; Pqq, pyrroloquinoline quinone; YT, yeast-tryptone; LB, Luria-Bertani; TFA, trifluoroacetic acid; BHI, brain-heart infusion; IR, infrared spectroscopy; NSM, new sporulation medium; THF, tetrahydrofuran.

ATCC 27899 with sodium [^{13}C]bicarbonate (99% isotopic purity) and sodium [^{15}N]nitrate (99% isotopic purity) as reported by Sailer et al (*25*) with the following differences. An oxygen gas electrode was excluded and a BioRad model EP-1 Econo peristaltic pump replaced the syringe pumps. Standing precultures of *Anabaena* sp., (2 × 500 mL) were inoculated with 10 mL of growing culture. After 12 days, the standing *Anabaena* cultures were centrifuged (15−20 min at 8000 rpm), the supernatant was discarded, and the cyanobacterial pellet was resuspended with a small amount of BG-11 media. The concentrated solution from 2 × 500 mL precultures was then added to 8 L of fermentation media. Subsequent fermentation and processing of the *Anabaena* algal cell mass followed the literature procedure. Four 8-L fermentations were grown and the percent of isotopic enrichment was determined as described below.

Determination of ^{13}C and ^{15}N Enrichment. A Carlo Erba EA1108 CHN Analyzer was coupled to a Hewlett-Packard (HP) Gas chromatograph (GC) (5890 series II) with a HP 5MS column (30 m × 0.25 mm × 0.25 μm film) and a HP Atomic Emission detector (AED) (5921A). Samples of peptone (1−3 mg) were subjected to normal combustion analysis on the CHN instrument and the vapor stream from these samples was fed directly into the GC-AED system. The GC-AED was set to monitor ^{12}C at 342.574 nm, ^{13}C at 341.712 nm, ^{14}N at 421.465 nm, and ^{15}N at 420.168 nm. Quantification for ^{12}C and ^{13}C isotopes was achieved using standards of *p*-chlorobenzoic acid and unlabeled and [^{13}C]-labeled succinic acid. Benzamide samples (^{15}N-labeled and unlabeled) were used as standards for ^{14}N and ^{15}N isotope analysis. All data were corrected for background and detector response. The amount of labeled peptone and percentages of ^{13}C and ^{15}N incorporated were as follows: fermentations A + B: 12.5 g, 100% ^{13}C, 83% ^{15}N; C: 17.9 g, 100% ^{13}C, 77% ^{15}N; D: 13.2 g, 100% ^{13}C, 81% ^{15}N. The percentage ratios of H:C:N were (5−6):(34−37):(9−10).

Production of Labeled Subtilosin A. A combined sample of labeled peptone (21 g) and 400 mL of milli-Q H_2O were added to each of two 2-L Erlenmeyer flasks and autoclaved at 121 °C for 15 min. One-half of a Quest "Once-a-day" vitamin (crushed with mortar and pestle) plus filter sterilized solutions of 0.5 g of $MgSO_4 \cdot H_2O$ and 2 g of KCl were then added. *B. subtilis* was grown and subtilosin A was purified as above, with the following alteration. The solution was centrifuged, the BuOH layer was carefully pipetted to a flask for evaporation, and the residual emulsion was reextracted with BuOH.

Labeling with [U-^{13}C,^{15}N]-Phenylalanine and [U-^{13}C,^{15}N]-Threonine. Subtilosin A was produced as above with the following adjustments. A culture (1.5 mL) of logarithmically growing cells of *B. subtilis* JH642 was transferred to 500 mL of NSM media (with no added glucose). [U-^{13}C,^{15}N]-L-Phenylalanine (1 g, 98% ^{13}C; 96−99% ^{15}N) was added at 0.5 g per 500 mL of NSM media. In a separate experiment, [U-^{13}C,^{15}N]-L-threonine (1 g, 98% ^{13}C; 96−99% ^{15}N) was added to 500 mL of NSM media. The cultures were shaken, incubated, and processed as above.

*Desulfurization of Subtilosin A to **14**.* $NaBH_4$ (7.5 mg) was added to a suspension of **1** (5 mg) and $NiCl_2$ (7.5 mg) in MeOH (3.75 mL) and mill-Q H_2O (2.5 mL) in a 15-mL pressure sealed tube, which was then immediately capped. The reaction was heated to 50 °C for 5 min, then an additional aliquot of $NaBH_4$ was added and the reaction was continued for another 5 min. A 100 μL aliquot was removed and acidified by adding 30 μL of TFA, then microcentrifuged for 1 min at 12 000 rpm. The extent of desulfurization was evaluated by MALDI-TOF, and additional aliquots of $NaBH_4$ and $NiCl_2$ were added as necessary to bring the reaction to completion. The mixture was then centrifuged for 10 min at 8000 rpm and purified by HPLC using a Waters C-18 Nova-Pak cartridge column with a 24 to 76% CH_3CN gradient over 20 min. The retention time (t_R) of **14** was 17 min. Fractions containing **14** were concentrated in vacuo and lyophilized. Mass spectral analysis of **14** using an Applied Biosystems Voyager Elite MALDI TOF system with delayed extraction and ion mirror (reflectron) gave M = 3311.1, corresponding to addition of six hydrogens with loss of three sulfurs from **1**.

*Hydrolysis of **14** and Formation N-Pentafluoropropanoyl Isopropyl Ester Derivatives of Constituent Amino Acids for GCMS Analysis.* Following desulfurization, the dry peptide **14** was derivatized according to Alltech GC reagent instructions included in the PFP-IPA Amino Acid Derivatization kit (Cat. No. 18093). Desulfurized **14** was hydrolyzed with acid and dried, esterified with a mixture of acetyl chloride and *i*-propanol and dried. This was followed by addition of the pentafluoropropanoyl group using pentafluoropropanoyl anhydride at 100 °C. After cooling of the mixture containing the derivatized amino acids, excess reagents and byproducts were evaporated under argon. The residue was redissolved in CH_2Cl_2 in preparation for chiral GC analysis (see Supporting Information) with an Alltech Heliflex Chirasil-Val Capillary column for the separation of optical isomers. Each injection was 1 μL with a concentration of 1 μg μL^{-1}. Standards were prepared separately in the same fashion using 20 mg each of L-Phe, D-Phe, L-Thr, and D-Thr. A mixture of L-amino acids (5 mg each of Ala, Ile, Lys, Trp, Gly, Phe, and Val) was also derivatized to evaluate efficiency of separation of the column and to prepare a library. Finally, a standard was prepared by hydrolysis and derivatization of insulin chain B (Sigma) by the same procedure.

*Partial Acid Hydrolysis of Desulfurized Subtilosin A (**14**).* A solution (1 mM) of desulfurized subtilosin A (**14**) (20 mg) in 0.1 N HCl was added to a 15 mL pressure sealed tube, which was then heated at 100 °C for 10 h. The sample was then concentrated in vacuo over NaOH. The peptide mixture was redissolved in MeOH (8 mL) and subjected to RP-HPLC using a Waters Nova-Pak C-18 cartridge column with a gradient of 20−80% CH_3CN over 60 min. Equivalently separated fractions were combined and reduced to a volume of 1 mL in a vacuum centrifuge. Each fraction was evaluated using electrospray LCMS (Agilent 1100 MSD) using a Phenomenex Luna 3 micron C-18 2 × 50 mm LC column. Peptide masses observed were compared to those predicted by PAWS (Protein Analysis WorkSheet) software for partially hydrolyzed **14**. The chosen fractions were then lyophilized, hydrolyzed, derivatized (to *N*-pentafluoropropanamide isopropyl esters), and analyzed employing chiral GC MS (injection volume 3 μL). This procedure used for the peptide fragments was analogous to that described above for complete hydrolysis and derivatization/analysis of **14**.

Synthesis of Model Compounds. Detailed protocols for the preparation of model compounds **3**−**13**, as depicted in

Scheme 1: Synthesis of Phenylalanine- and Threonine-Derived Model Compounds and ^{13}C Chemical Shift Values for Their α-Carbons[a]

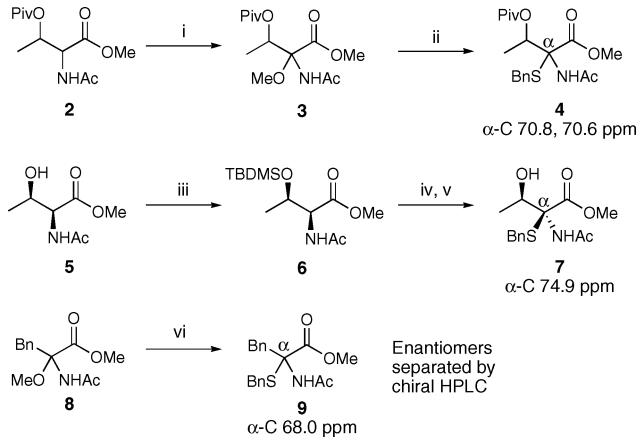

[a] Reagents and conditions: i, *t*-BuOCl, NaOMe, MeOH, 0 °C → rt, 60 min, 92%; ii, BnSH, $SnCl_4$, CH_3CN, 0 °C → rt, 16 h, 68%; iii, TBDMSCl, DMF, imidazole, 40 °C, 16 h, 92%; iv, *t*-BuOCl, NaOMe, MeOH, 0 °C → rt, 60 min; v, BnSH, $SnCl_4$, CH_3CN, 0 °C → rt, 5 h, 2%; vi, BnSH, $SnCl_4$, CH_3CN, 0 °C → rt, 105 min, quant.

Scheme 2: Nickel Boride Reductions of **4**, **7**, and **9**[a]

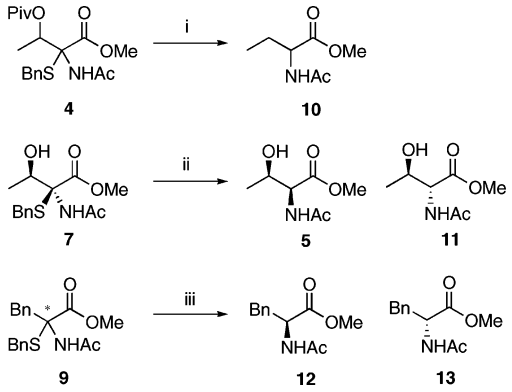

[a] Reagents and conditions: i, $NaBH_4$, $NiCl_2$, MeOH, rt, 5 min, quant.; ii, $NaBH_4$, $NiCl_2$, MeOH, 0 °C, 15 min, quant.; iii, $NaBH_4$, $NiCl_2$, MeOH, 50 °C, 3 h, quant.

Schemes 1 and 2, are presented in the Supporting Information.

NMR Spectroscopy. All samples for NMR spectroscopy used 500 μL of degassed CD_3OH (Sigma) and 5-mm high quality Wilmad NMR tubes, and all solvents and solutions were kept under argon. A suite of one-, two-, and three-dimensional homo- and heteronuclear experiments were conducted at 15 °C on either a Varian Inova-500 or Inova-800 MHz spectrometer, and were referenced to DSS (*26*). All experiments were processed using the software package NMRPipe (*27*) and analyzed using the program NMRView (*28*) with substantial in-house modifications available upon request (http://www.nanuc.ca). Linear prediction was used to increase the number of points in the indirectly detected dimensions by up to half the number of acquired points, and zero filling was used to extend both the directly and indirectly detected dimensions to twice the number of acquired plus predicted points. Spectra were apodized using a $\pi/2$ or $\pi/3$ shifted sine bell before Fourier transformation.

Structure Calculations. Eight rounds of ARIA (*29*), using NOESY peaks from a ^{13}C-HSQC-NOESY and ^{15}N-HSQC-NOESY were carried out for each of the eight possible stereoisomers of subtilosin A. The restraints generated by ARIA were then used to calculate 50 more structures for each stereoisomer, using CNS 1.1 (*30*) to further compare the differences in energy and rmsd of the accepted structures. The LDD stereoisomer, which consistently gave the lowest energy structures, was further refined using a dynamical annealing procedure in CNS 1.1. A total of 301 unique NOEs resulting from the ARIA calculations and 20 dihedral angle restraints (*31*) were used as constraints. Eight lowest-energy structures, with no residues in the disallowed regions of the Ramachandran plot, of 50 calculated were chosen to represent the solution structure of subtilosin A in MeOH.

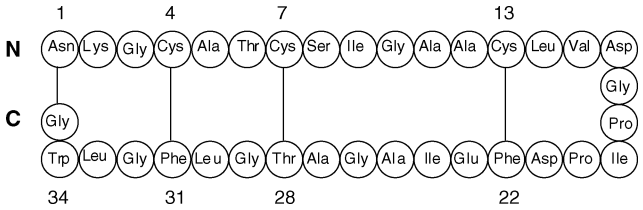

FIGURE 1: Amino acid sequence of subtilosin A (**1**). The positions of the posttranslationally formed linkages are indicated by solid lines.

RESULTS AND DISCUSSION

The mature subtilosin peptide is highly resistant to enzymatic proteolysis and is stable to moderate heat and acid treatment. The first reported attempts to sequence the peptide and determine the nature of its posttranslational modifications were only partially successful in obtaining the correct amino acid sequence and structure (*17*). It defies complete sequence analysis by Edman degradation or mass spectral examination, even after partial acid hydrolysis into fragments. Identification of the genetic locus for subtilosin production allowed prediction of the amino acid sequence (*18*). However, the monoisotopic mass of isolated **1** is 3401.2 ± 0.5 Da, and differs from the calculated mass, 3426 Da, by 24−25 units. This is consistent with the loss of water during cyclization of the N and C termini, plus the loss of six hydrogens. Although two phenylalanine and two threonine residues are encoded by the genetic sequence, only one threonine and no phenylalanines were found by amino acid analysis of purified **1** (*17*, *18*). It was proposed that linkages could exist between the cysteine residues at positions 4, 7, and 13 and Phe31, Thr28, and Phe22, respectively (*19*), (Figure 1) which would correspond to the loss of a hydrogen from each of these six residues. Such residue proximities were included in a proposed NMR solution structure by Marx et al (*19*), but the exact connectivity remained uncertain, with bonds between sulfur and the aromatic rings of Phe22 and Phe31, as well as between sulfur and the β-carbon of Thr28 being suggested. Since the cross-links could not be determined, the proposed 3D structures (*19*) are not accurate. Like other bacteriocins, subtilosin A could not be crystallized for X-ray analysis, despite extensive attempts. To elucidate the exact position of the cysteine sulfur−phenylalanine and threonine bonds, NMR studies on ^{13}C,^{15}N-labeled subtilosin A were undertaken.

Labeling of Subtilosin A and NMR Assignment: Analysis of the Cysteine-Phenylalanine and Cysteine-Threonine Bonds. Initial NMR investigation of **1** indicated that labeling with ^{13}C and ^{15}N was essential due to extensive resonance overlap,

which precluded unambiguous assignment of all signals. Although *B. subtilis* can be grown under a variety of conditions, significant production of this target peptide (5−10 mg per liter) could only be obtained on complex media described earlier (*18*) and on a peptone-based formulation derived from a cyanobacterium, *Anabaena* sp. (*25*). Use of commercially available algal-derived peptones was not successful in generating substantial levels of the desired peptide. Hence, universally [^{13}C,^{15}N]-enriched subtilosin A was prepared by fermentation of *B. subtilis* JH642 on a labeled peptone media that was generated from 32 L (4 × 8 L) of blue green algae (*Anabaena* sp. ATCC 27899) grown on sodium [^{13}C]bicarbonate and sodium [^{15}N]nitrate as the sole carbon and nitrogen sources (*25*). Levels of isotopic labeling of the peptone samples were determined to be 85−98% ^{13}C and 77−95% ^{15}N using an unconventional method, namely, combustion of small samples using elemental (CHN) analysis equipment coupled with atomic emission determination of ^{12}C/^{13}C and ^{14}N/^{15}N ratios in the resulting gaseous products. Some variation of labeling levels is observed in the peptone due to different amounts of unlabeled innoculum (preculture) used to initiate the *Anabaena* fermentation. Electrospray mass spectral analysis of the labeled **1** derived from *B. subtilis* cultures grown in this peptone medium indicated comparable levels of labeling in the peptide.

Backbone carbon, nitrogen, and proton assignments for the 35-amino acid cyclic peptide were determined using a standard panel of NMR experiments, including HNCACB and CBCACONH (see Supporting Information). Spectra were recorded in methanol-d_3, due to the insolubility of subtilosin A in aqueous solvent. Interestingly, the chemical shifts for the α-carbons of Phe22, Thr28, and Phe31 are downfield of compilation values (*32*) by approximately 10 ppm, which is consistent with the influence of an electronegative atom such as sulfur being directly attached. Model compounds **4**, **7**, and **9** were also prepared (Scheme 1), and their α-carbon chemical shifts agree with those observed for the modified residues in subtilosin A (**1**). Complete assignment of all carbon, nitrogen, and proton chemical shifts (including side chains) indicated that indeed these α-carbons are fully substituted. To confirm that the amino acid assignments are correct, universally labeled [^{13}C,^{15}N]-L-phenylalanine and [^{13}C,^{15}N]-L-threonine were added to separate fermentations of *B. subtilis* in unlabeled media. ^{13}C-COSY experiments on the selectively labeled subtilosin A preparations verified that the resonances at 69.4, 69.8, and 72.8 ppm correspond to the α-carbons of Phe22, Phe31, and Thr28, respectively (Figure 2). The absence of cross-peaks at these chemical shifts in ^{1}H,^{13}C-HSQC spectra further illustrates that the thioether linkage consists of an unusual sulfur-α-carbon bond. Analysis of long range ^{1}H-^{1}H NOEs observed for the modified residues unambiguously identified the amino acids involved in each thioether bond (Figure 3). The *β*-protons of Cys4 show NOEs to the amide proton of Phe31 and the amide and alpha protons of Gly32. Similarly NOEs are observed between Cys7 and Thr28 and Gly29. The only long-range NOEs involving Cys13 are to Glu23. The α-carbons of the modified amino acids Phe22, Thr28, and Phe31 are bonded to Cys13, Cys7, and Cys4, respectively.

This type of posttranslational modification, namely, oxidative linkage of cysteine sulfur to the α-carbon of another amino acid residue, has not been previously observed in any other *ribosomally synthesized* peptide. Cyclothiazomycin, a *nonribosomal* peptide from *Streptomyces* with renin inhibitory activity, is a rare example that has cysteine sulfur linked to the α-carbon of an alanine with inversion of configuration at that center (*33*, *34*). The other close analogy to such modifications occurs in fungal diketopiperazines, such as gliotoxins, aranotins, and sporidesmins (*35*, *36*). However,

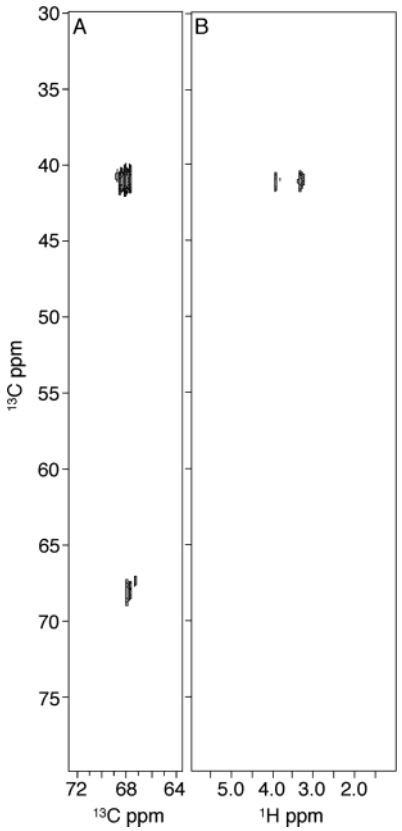

FIGURE 2: NMR spectra of U-[^{13}C,^{15}N]Phe-labeled subtilosin A. (A) ^{13}C-COSY showing Phe Cα−C*β* correlations. (B) ^{1}H,^{13}C-HSQC demonstrating that only the C*β*s have attached protons. The Cα and C*β* resonances of Phe22 and Phe31 are nearly overlapped. Spectra recorded at 500 MHz.

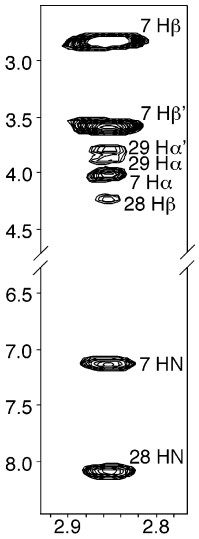

FIGURE 3: ^{1}H−^{1}H strip from a ^{13}C HSQC-NOESY displaying NOE correlations between Cys7 H*β* and Thr28. Spectrum recorded at 800 MHz.

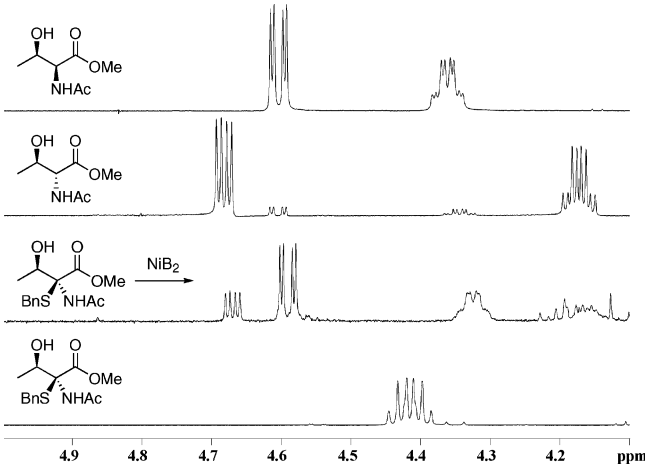

FIGURE 4: ^{1}H NMR analysis of desulfurization of threonine derivative **7** with nickel boride. From top 500 MHz NMR spectra of *N*-acetyl-L-threonine methyl ester; *N*-acetyl-D-allo-threonine methyl ester; products of NiB_2 reduction of **7** indicating a mixture of the above two compounds; starting material **7**.

in these eukaryotic secondary metabolites the presence of disulfide and trisulfide bridges, as well as thiomethyl adducts, suggests that sulfur donor(s) other than cysteine and different mechanisms may be involved.

Synthesis and Desulfurization of Model Compounds. Model compounds **4**, **7**, and **9** were initially synthesized as shown in Scheme 1 to examine the chemical shifts at the α-carbons as described above. The approach relies on the well-established oxidation of N-acyl α-amino acid esters to highly reactive intermediate N-acyl imines, which then add nucleophiles such as methanol (*37*). Treatment of the methoxy compounds with benzyl thiol in the presence of tin tetrachloride allows the in situ regeneration of the N-acyl imine under nonoxidative conditions (*38*), which then undergoes rapid nucleophilic addition to form the corresponding sulfides **4**, **7**, and **9**, which represent a new class of molecules. This procedure causes loss of stereochemistry at the α-carbon. However, in the case of the L-threonine derivative **6**, the stereocontrol exerted by the configuration at the *β*-carbon results in generation of only one enantiomer of **7**, whose absolute stereochemistry was determined by X-ray crystallography (see Supporting Information). The enantiomers of **9** could be separated by HPLC on a chiral support, but extensive attempts to obtain a crystallographic structure were not successful.

Elegant studies on nickel boride desulfurization, in particular, of steroidal sulfides, clearly demonstrated that such replacement of sulfur by hydrogen generally proceeds with retention of configuration (*39*). Hence, it appeared that this reaction might be an effective probe of the stereochemistry of the sulfur to α-carbon linkages in subtilosin A. We first examined the outcome of the nickel boride desulfurization reaction with compounds **4**, **7**, and **9** (Scheme 2).

The O-protected threonine derivative **4** lost both the thioether and pivalate groups. In contrast, the threonine derivative **7** having a free hydroxy group, as well as the phenylalanine analogue **9**, could be successfully desulfurized to generate the *N*-acetylated amino acids. However, a mixture of diastereomers results from desulfurization of **7**, as can readily be observed by ^{1}H NMR (Figure 4).

Similar treatment of enantiomerically pure **9**, prepared by a HPLC separation on a chiral support (Chiracel OJ), generates a racemic mixture of phenylalanine derivatives **12** and **13** (see Supporting Information). Thus, desulfurization of both the threonine and phenylalanine derivatives proceeds with epimerization at the α-carbon. Careful examination of the literature indicates that desulfurization of 3-aryl-3-phenylthioflavanones also results in loss of stereochemical integrity (Figure 5) (*40*). It appears that in this case the reaction proceeds by elimination of thiol followed by reduction of the planar achiral α,*β*-unsaturated ketone. We propose that in our model systems the thiol is similarly first eliminated to form a reactive planar N-acyl imine, which is then reduced to an amine in a nonstereospecific fashion.

Desulfurization and Hydrolysis of Subtilosin A. Although the nickel boride desulfurization results in epimerization for the model compounds **7** and **9** (in contrast to the normally observed retention of configuration for simple sulfides), in subtilosin A (**1**) the bridged structure could make one face of the intermediate N-acyl imine more accessible to reduction. It also seemed that desulfurization of this highly modified peptide could assist hydrolytic cleavage of the peptide backbone for sequencing as well as analysis of stereochemistry of the ostensibly unmodified amino acid residues. As mentioned above, both hydrolysis and amino acid sequencing of subtilosin A was problematic (*16*, *17*). Nickel boride desulfurization to **14** was successful in reductive cleavage of the thioether bridges, with regeneration of the parent residues Phe22, Phe31, and Thr28, as well as conversion of Cys13, Cys7, and Cys4 to alanine residues (Figure 6) (*39*, *41*, *42*). These sulfide bridges are necessary for antimicrobial activity, as the desulfurized compound **14** is inactive (data not shown).

Following desulfurization, the resulting **14** was submitted to complete acid hydrolysis and conversion of the constituent amino acids to *N*-pentafluoropropanamide isopropyl esters for chiral GC MS analysis. The stereochemistry of all the unmodified residues could thus be examined and was determined to be L. Threonine was detected as the L stereoisomer only, and a mixture of D and L stereochemistries was observed for phenylalanine. Since there is an unmodified threonine residue at position 6 and a modified threonine at position 28 in **1**, the desulfurization and subsequent hydrolysis experiments show that desulfurization of Thr28 proceeds with complete stereochemical selectivity. Detailed NMR analysis of subtilosin A (see below) shows that prior to reductive desulfurization the modified Thr28 is D (S configuration due to priority change). The results demonstrate that the desulfurization of this residue proceeds with net *inversion* of configuration, presumably by formation of the corresponding N-acyl imine under the basic conditions followed by hydride delivery from the less hindered exterior face of the cyclic peptide.

To determine the stereochemical outcome of reduction of the two modified phenylalanines, a limited hydrolysis with 0.1 N HCl was done on **14** to afford larger peptide fragments, which were separated by HPLC. Although such hydrolysis of the parent subtilosin A does not give large fragments amenable to Edman (or mass spectrometric) sequencing, the desulfurized compound **14** can be cleaved with moderate selectivity at less sterically crowded glycine residues. A fragment with a mass of 1015.5 Da was isolated, corre-

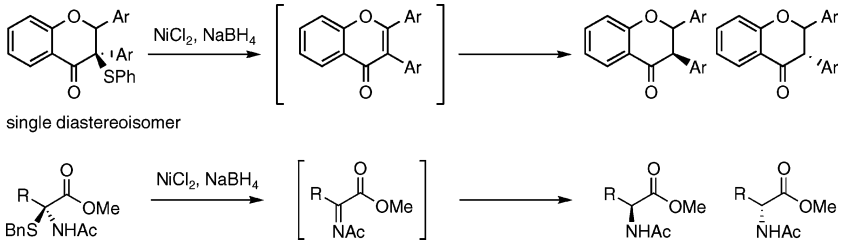

FIGURE 5: Proposed elimination−reduction mechanism for epimerization during NiB_2 desulfurizations of 3-aryl-3-phenylthioflavanones and α-thiol-*N*-acyl amino acids.

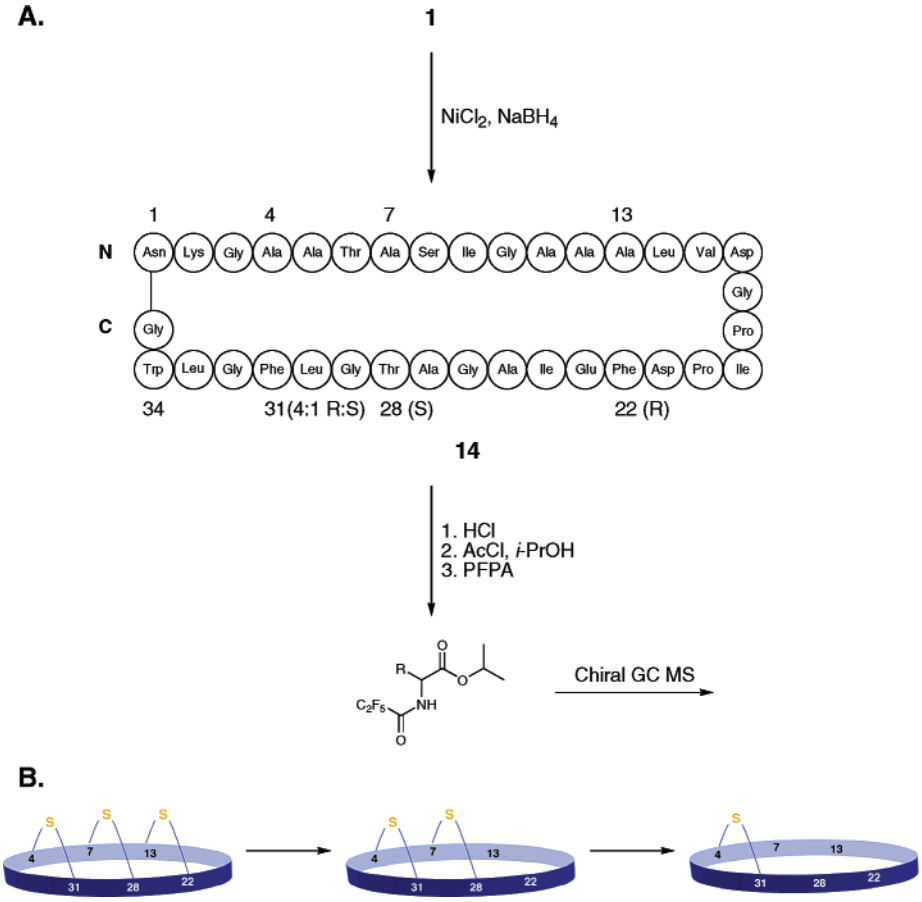

FIGURE 6: (A) Reductive cleavage of thioether bridges of subtilosin A (**1**) to form **14** followed by complete hydrolysis and derivatization to determine residue stereochemistry. (B) Proposed sequence of reductive desulfurizations.

sponding to residues 17−26 (Gly-Pro-Ile-Pro-Asp-Phe-Glu-Ile-Ala-Gly), which contains Phe22. Two fragments containing Phe31 were also separated: one with a mass of 692.4 Da, corresponding to residues 29−34 (Gly-Leu-Phe-Gly-Leu-Trp);[2] and another with mass of 635.4 Da, corresponding to residues 30−34 (Leu-Phe-Gly-Leu-Trp). Each of these peptides was separately hydrolyzed to constituent amino acids, which were then converted to *N*-pentafluoropropanamide isopropyl esters for chiral GC MS analysis as before. The results show that in desulfurized compound **14**, within experimental error, Phe22 has exclusively D configuration, whereas Phe31 exists as a 4:1 mixture of D:L. NMR studies of **1** (see below) show that the modified Phe22 is L (R configuration because of priority change) and that modified Phe31 is D (S). Hence, nickel boride reduction of **1** proceeds with *inversion* of configuration at Phe22 (a stereochemical outcome in agreement with the reduction of modified Thr28) and with 4:1 *retention* at Phe31.

Taken together with the desulfurization of the model compounds, which proceeds with complete racemization, these results show that amino acid residues having a sulfide substituent at the α-carbon first suffer elimination of thiolate under the basic nickel boride conditions and then the resulting N-acyl imine is reduced with stereochemical preference being controlled by the geometry of the peptide. During desulfurization, it was noted that two sulfurs are relatively easy to remove, (Cys7−Thr28; Cys13−Phe22) but the last sulfur (Cys4−Phe31) requires much longer reaction times and extra additions of $NiCl_2/NaBH_4$. This suggests that the desulfurization process "unzips" the bowl-like molecule **1** (see below) from the Cys13−Phe22 end, with the first two reductions

[2] This fragment could also contain residues 30−35 (Leu-Phe-Gly-Leu-Trp-Gly). The two possibilities were not distinguished because each contains only Phe31, whose isolation was the goal of this analysis.

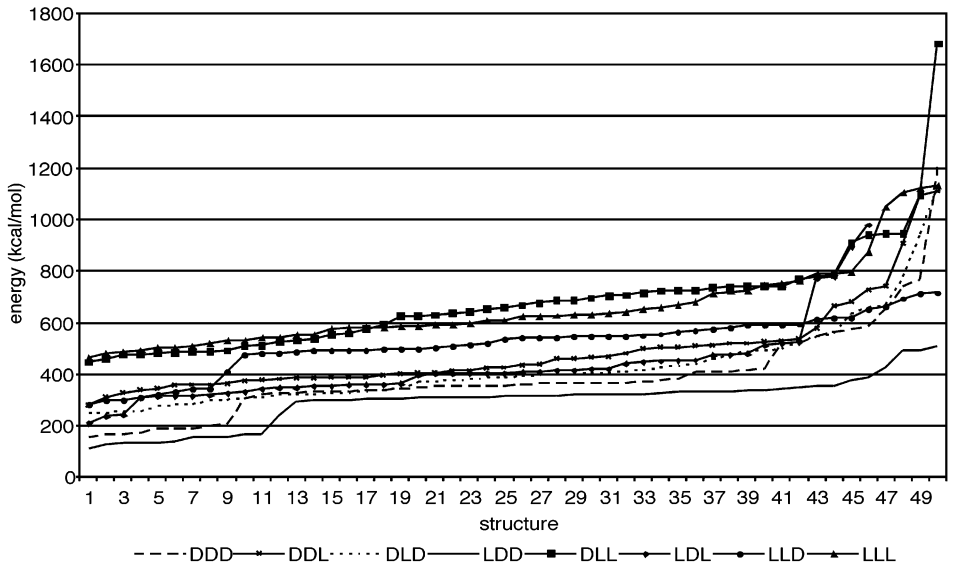

FIGURE 7: Plot of overall energy versus structure number for the 50 structures calculated for each possible stereoisomer of subtilosin A.

occurring from the "exterior" surface, and the last reduction proceeding predominantly from what was the "interior" of the now opened bowl (Figure 6B).

NMR Solution Structure. Since the stereochemistry of the three modified residues in **1** could not be directly established by chemical degradation experiments, NMR structure determination was used to analyze the configuration at each of these stereocenters. ^{13}C-HSQC-NOESY, ^{15}N-HSQC-NOESY, and HNHA experiments were recorded for universally ^{13}C,^{15}N-labeled subtilosin A. Each of the eight possible stereoisomers of subtilosin A were submitted to eight rounds of ARIA calculations, starting with the same peak files and assignments. Similar NOE assignments were obtained for each stereoisomer; however, the overall energies for each group of 20 structures varied. A further 50 structures for each stereoisomer were generated with CNS using the restraints assigned by ARIA (see Experimental Section). The stereoisomer with the L configuration at Phe22 and D stereochemistries at Thr28 and Phe31 (LDD) consistently fit the NMR data the best, giving the lowest energy family of structures with the best rmsd (Figure 7). The DDD isomer, the next best, does not match the NOE data as well, and the structures calculated for the six remaining stereoisomers increase in energy and rmsd.

The structure for the LDD stereoisomer of subtilosin A was further refined, using a total of 301 unique NOEs and 20 dihedral angle restraints (Table 1). A family of eight structures of subtilosin A was chosen to represent its conformation in methanol. Subtilosin A forms a twisted, bowl-like structure, with most side chains pointing toward the solvent (Figure 8). The backbone rmsd for the final family of structures is 2 Å. This relatively large value is due to a paucity of medium and long-range NOEs, as most of the side chains point outward, and there is a large proportion of glycines in the sequence. Almost all of the long-range NOEs observed arise from residues brought together by the thioether bonds. The center of the molecule, bordered by the Cys4−Phe31 and Cys13−Phe22 cross-links, is therefore better defined, with a backbone rmsd of 1.2 Å.

The sulfide bridges are necessary for the antimicrobial activity of subtilosin A, and constrain the central portion of the structure, while allowing a degree of motional freedom to the side chains and end loops. The high number of hydrophobic amino acids, which point toward the solvent, explains why subtilosin A is nearly insoluble in aqueous solutions. Many of the antibacterial peptides whose three-dimensional structures have been determined are unstructured or insoluble in water, and only form regular secondary structure in membrane mimetic or polar solvents (*10*, *43*−*46*). Since the bactericidal activity of these peptides is exerted at the level of the membrane, either by direct insertion and/or binding to cell surface receptors (*2*, *6*−*12*, *47*), it is reasonable to argue that NMR structures determined in nonaqueous systems are representative of biologically rel-

Table 1: Statistics for Structure Calculations

total NOE restraints	301
intraresidue	163
sequential ($\|i-j\|=1$)	78
medium range ($1<\|i-j\|\leq 4$)	30
long range ($\|i-j\|>4$)	27
dihedral angle restraints	20
statistics for structure calculation	⟨SA⟩[a]
rmsd from idealized covalent geometry	
bonds (Å)	0.0024 ± 0.0002
bond angles (°)	0.37 ± 0.01
improper torsions (°)	0.28 ± 0.02
rmsd from experimental distances (Å)[b]	$0.014 \pm .002$
final energies (kcal mol^{-1})	
E_{total}	57.9 ± 5.3
E_{bonds}	2.8 ± 0.3
$E_{impropers}$	3.0 ± 0.5
E_{vdW}[c]	27.2 ± 3.3
E_{NOE}	4.4 ± 1.2
coordinate precision[d] (Å)	⟨SA⟩ versus $\langle\overline{SA}\rangle$
rmsd of all backbone atoms (N, Cα, C′)	2.0 ± 0.5
rmsd of all heavy atoms	2.8 ± 0.5
rmsd of all backbone atoms, residues 4−13 and 22−31	1.2 ± 0.4
rmsd of all heavy atoms, residues 4−13 and 22−31	1.8 ± 0.3

[a] ⟨SA⟩ refers to the ensemble of eight structures. [b] No NOEs were violated by more than 0.15 Å. [c] Repel = 1.0 for the final step of calculations. [d] rmsd between the ensemble of structures ⟨SA⟩ and the average structure of the ensemble $\langle\overline{SA}\rangle$.

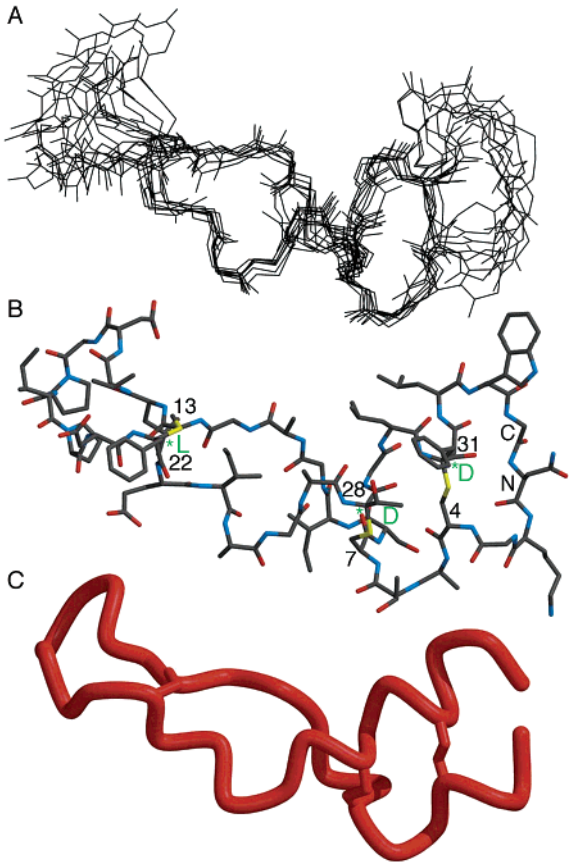

FIGURE 8: (A) Superposition on the backbone of residues 4−13 and 22−31 of the eight lowest energy structures of subtilosin A. (B) Representative conformer of subtilosin A in the same orientation, illustrating the outward pointing side chains. The positions and stereochemistry of the cross-links are indicated. (C) Coil representation of the backbone of subtilosin A; a break is shown at the position of the C−N terminal cyclization.

evant conformations. In contrast to many bacteriocins, which have an overall positive charge at physiological pH, subtilosin A has only one lysine and a total of three aspartate and glutamate residues. This suggests that it may not interact solely with the cell membrane, and may possibly first bind to a surface receptor. The sulfide bridges may hold it in a conformation which easily adapts to its target molecule.

CONCLUSIONS

We have identified a novel type of posttranslational modification, namely, a sulfur to α-carbon cross-link, in the bacteriocin subtilosin A (**1**). Such cross-links are necessary for its antimicrobial activity, and hold the peptide in a twisted, bowl-like conformation in methanol, with most of the side chains pointing toward the solvent. The configurations of the unmodified amino acids are all L, whereas those of the modified residues are L-Phe22, D-Thr28, and D-Phe31 based on extensive NMR analysis. This means that the biochemical formation of the sulfur to α-carbon cross-links proceeds with net retention of configuration at Phe22, and with net inversion at Thr28 and Phe31. Inspection of the NMR structures reveals that a twist in the structure renders the opposite face of the Cys13−Phe22 bond accessible in comparison to the Cys7−Thr28 and Cys4−Phe31 bonds. This orientation may be favored during the maturation of subtilosin A, resulting in the different chiralities at the modified amino acids. The enzymatic mechanism that is responsible for this unusual posttranslational mechanism is not yet known. However, it is possible that the process involves attack of a nearby cysteine thiol on a highly reactive N-acyl imine moiety, in analogy to the final step in the chemical synthesis of model compounds **4**, **7**, and **9**. It is presently unclear whether such N-acyl imines are formed directly by enzymatic dehydrogenation or by a sequence of N-hydroxylation followed by elimination (*35*, *36*). Although hydroxylation of the α-carbon followed by elimination could in principle also generate such an imine, this seems less likely as the intermediate hydroxy species would probably form an α-keto amide. Two of the genes in the *sbo-alb* locus of *B. subtilis*, *albA* and *albF*, are critical for production of mature subtilosin A (*48*). Homology between the *albA* gene product and members of the MoaA/NifB/PqqE family, which contain Cys clusters that bind Fe−S complexes (*49*, *50*), suggests that this enzyme or one(s) which it generates may catalyze the oxidation reactions during the posttranslational modification of the presubtilosin. The *albA* gene product is homologous to radical SAM enzymes (*51*). Hence, an adenosyl radical could form the Cys−Phe and Cys−Thr linkages, possibly via a diradical mechanism that does not directly involve an N-acyl imine. The N-terminal half of AlbF demonstrates sequence similarity to mitochondrial metalloproteases associated with the cytochrome bc_1 complex (*52*−*54*). Identification of the products of these genes should yield insights into the mechanism of this novel posttranslational modification, and could lead to discovery of other previously unknown thioether linkages in bacteriocins.

Investigation of the nickel boride reductive desulfurization of **1**, as well as of the model compounds **4**, **7**, and **9**, indicates that base-induced elimination to form an N-acyl imine occurs first followed by reduction to the amide. This leads to complete racemization for the model compounds, but the stereochemical outcome with **1** is governed by accessibility of the polymeric reducing agent to the relatively rigid peptide scaffold. This is in contrast to the usual retention of configuration observed with systems that have no acidic hydrogens on the atom adjacent to the carbon bearing sulfur. The combination of nickel boride reduction of a sulfur-containing peptide and Edman sequence analysis is a powerful tool for structure elucidation of posttranslationally modified peptides. Further studies on this methodology and on the biosynthetic machinery for production of **1** are in progress.

ACKNOWLEDGMENT

We thank Leon Lau and Liang-Zeng Yan for development of purification procedures for subtilosin A, James Hoyle for atomic emission analyses of isotopic content, Robert McDonald for x-ray analyses, and Leo Spyracopoulos for access to his computers.

SUPPORTING INFORMATION AVAILABLE

Preparations and spectral data of compounds **3**−**13**; chiral HPLC analysis of the desulfurization of **9a**; crystal structure of **7**; chemical shifts for subtilosin A (also available from the BioMagResBank (BMRB code 5860)); HN NOE, t1 and t2 data for subtilosin A; chiral GC MS analysis for complete hydrolysis and derivatization of **14** and partial hydrolysis fragments 1−3. This material is available free of charge via the Internet at http://pubs.acs.org.

REFERENCES

1. Nes, I. F., and Holo, H. (2000) Class II antimicrobial peptides from lactic acid bacteria. *Biopolymers 55*, 50−61.
2. van Belkum, M. J., and Stiles, M. E. (2000) Nonlantibiotic antibacterial peptides from lactic acid bacteria. *Nat. Prod. Rep. 17*, 323−335.
3. Nilsen, T., Nes, I. F., and Holo, H. (2003) Enterolysin A, a cell wall-degrading bacteriocin from *Enterococcus faecalis* LMG 2333. *Appl. Environ. Microbiol. 69*, 2975−2984.
4. van Kraaij, C., de Vos, W. M., Siezen, R. J., and Kuipers, O. P. (1999) Lantibiotics: biosynthesis, mode of action and applications. *Nat. Prod. Rep. 16*, 575−587.
5. Guder, A., Wiedemann, I., and Sahl, H. G. (2000) Posttranslationally modified bacteriocins- the lantibiotics. *Biopolymers 55*, 62−73.
6. McAuliffe, O., Ross, R. P., and Hill, C. (2001) Lantibiotics: structure, biosynthesis and mode of action. *FEMS Microbiol. Rev. 25*, 285−308.
7. Moll, G. N., Konings, W. N., and Driessen, A. J. (1999) Bacteriocins: mechanism of membrane insertion and pore formation. *Antonie Van Leeuwenhoek 76*, 185−198.
8. Wiedemann, I., Breukink, E., van Kraaij, C., Kuipers, O. P., Bierbaum, G., de Kruijff, B., and Sahl, H. G. (2001) Specific binding of nisin to the peptidoglycan precursor lipid II combines pore formation and inhibition of cell wall biosynthesis for potent antibiotic activity. *J. Biol. Chem. 276*, 1772−1779.
9. Breukink, E., van Heusden, H. E., Vollmerhaus, P. J., Swiezewska, E., Brunner, L., Walker, S., Heck, A. J., and de Kruijff, B. (2003) Lipid II is an intrinsic component of the pore induced by nisin in bacterial membranes. *J. Biol. Chem. 278*, 19898−19903.
10. Hsu, S. T., Breukink, E., Bierbaum, G., Sahl, H. G., de Kruijff, B., Kaptein, R., van Nuland, N. A., and Bonvin, A. M. (2003) NMR study of mersacidin and lipid II interaction in dodecylphosphocholine micelles. Conformational changes are a key to antimicrobial activity. *J. Biol. Chem. 278*, 13110−13117.
11. Dalet, K., Cenatiempo, Y., Cossart, P., and Hechard, Y. (2001) A sigma(54)-dependent PTS permease of the mannose family is responsible for sensitivity of *Listeria monocytogenes* to mesentericin Y105. *Microbiology 147*, 3263−3269.
12. Hechard, Y., and Sahl, H. G. (2002) Mode of action of modified and unmodified bacteriocins from Gram-positive bacteria. *Biochimie 84*, 545−557.
13. Sahl, H. G., and Bierbaum, G. (1998) Lantibiotics: biosynthesis and biological activities of uniquely modified peptides from gram-positive bacteria. *Annu. Rev. Microbiol. 52*, 41−79.
14. Ross, R. P., Morgan, S., and Hill, C. (2002) Preservation and fermentation: past, present and future. *Int. J. Food Microbiol. 79*, 3−16.
15. Delves-Broughton, J., Blackburn, P., Evans, R. J., and Hugenholtz, J. (1996) Applications of the bacteriocin, nisin. *Antonie Van Leeuwenhoek 69*, 193−202.
16. Zheng, G., and Slavik, M. F. (1999) Isolation, partial purification and characterization of a bacteriocin produced by a newly isolated *Bacillus subtilis* strain. *Lett. Appl. Microbiol. 28*, 363−367.
17. Babasaki, K., Takao, T., Shimonishi, Y., and Kurahashi, K. (1985) Subtilosin A, a new antibiotic peptide produced by *Bacillus subtilis* 168: isolation, structural analysis, and biogenesis. *J. Biochem. (Tokyo) 98*, 585−603.
18. Zheng, G., Yan, L. Z., Vederas, J. C., and Zuber, P. (1999) Genes of the sbo-alb locus of *Bacillus subtilis* are required for production of the antilisterial bacteriocin subtilosin. *J. Bacteriol. 181*, 7346−7355.
19. Marx, R., Stein, T., Entian, K. D., and Glaser, S. J. (2001) Structure of the *Bacillus subtilis* peptide antibiotic subtilosin A determined by ^{1}H NMR and matrix assisted laser desorption/ionization time-of-flight mass spectrometry. *J. Protein Chem. 20*, 501−506.
20. Kawulka, K., Sprules, T., McKay, R. T., Mercier, P., Diaper, C. M., Zuber, P., and Vederas, J. C. (2003) Structure of subtilosin A, an antimicrobial peptide from *Bacillus subtilis* with unusual posttranslational modifications linking cysteine sulfurs to alpha-carbons of phenylalanine and threonine. *J. Am. Chem. Soc. 125*, 4726−4727.
21. Perrin, D. D., Aramarego, W. L. F., and Perrin, D. R. (1980) *Purification of Laboratory Chemicals*, 2nd ed., Pergamon Press, New York.
22. Still, W. C., Kahn, M., and Mitra, A. (1978) Rapid Chromatographic Technique for Preparative Separations with Moderate Resolution. *J. Org. Chem. 43*, 2923−2925.
23. Harwood, C. R., and Cutting, S. M. (1990) in *Molecular Biological Methods for Bacillus*, John Wiley & Sons, Chichester, U. K.
24. Korch, C. T., and Doi, R. H. (1971) Electron microscopy of the altered spore morphology of a ribonucleic acid polymerase mutant of *Bacillus subtilis*. *J. Bacteriol. 105*, 1110−1118.
25. Sailer, M., Helms, G. L., Henkel, T., Niemczura, W. P., Stiles, M. E., and Vederas, J. C. (1993) ^{15}N- and ^{13}C-labeled media from *Anabaena sp.* for universal isotopic labeling of bacteriocins: NMR resonance assignments of leucocin A from *Leuconostoc gelidum* and nisin A from *Lactococcus lactis*. *Biochemistry 32*, 310−318.
26. Wishart, D. S., Bigam, C. G., Yao, J., Abildgaard, F., Dyson, H. J., Oldfield, E., Markley, J. L., and Sykes, B. D. (1995) ^{1}H, ^{13}C and ^{15}N chemical shift referencing in biomolecular NMR. *J. Biomol. NMR 6*, 135−140.
27. Delaglio, F., Grzesiek, S., Vuister, G. W., Zhu, G., Pfeifer, J., and Bax, A. (1995) NMRPipe: a multidimensional spectral processing system based on UNIX pipes. *J. Biomol. NMR 6*, 277−293.
28. Johnson, B. A., and Blevins, R. A. (1994) NMR View − a Computer-Program for the Visualization and Analysis of NMR Data. *J. Biomol. NMR 4*, 603−614.
29. Nilges, M., Macias, M. J., O'Donoghue, S. I., and Oschkinat, H. (1997) Automated NOESY interpretation with ambiguous distance restraints: the refined NMR solution structure of the pleckstrin homology domain from beta-spectrin. *J. Mol. Biol. 269*, 408−422.
30. Brunger, A. T., Adams, P. D., Clore, G. M., DeLano, W. L., Gros, P., Grosse-Kunstleve, R. W., Jiang, J. S., Kuszewski, J., Nilges, M., Pannu, N. S., Read, R. J., Rice, L. M., Simonson, T., and Warren, G. L. (1998) Crystallography & NMR system: A new software suite for macromolecular structure determination. *Acta Crystallogr., Sect. D: Biol. Crystallogr. 54*, 905−921.
31. Wang, A. C., and Bax, A. (1996) Determination of the backbone dihedral angles phi in human ubiquitin from reparametrized empirical Karplus equations. *J. Am. Chem. Soc. 118*, 2483−2494.
32. Wishart, D. S., and Sykes, B. D. (1994) The ^{13}C chemical-shift index: a simple method for the identification of protein secondary structure using ^{13}C chemical-shift data. *J. Biomol. NMR 4*, 171−180.
33. Aoki, M., Ohtsuka, T., Itezono, Y., Yokose, K., Furihata, K., and Seto, H. (1991) Structure of Cyclothiazomycin, a Unique Polythiazole-Containing Peptide with Renin Inhibitory Activity. 2. Total Structure. *Tetrahedron Lett. 32*, 221−224.
34. Aoki, M., Ohtsuka, T., Yamada, M., Ohba, Y., Yoshizaki, H., Yasuno, H., Sano, T., Watanabe, J., Yokose, K., and Seto, H. (1991) Cyclothiazomycin, a novel polythiazole-containing peptide with renin inhibitory activity. Taxonomy, fermentation, isolation and physicochemical characterization. *J. Antibiot. (Tokyo) 44*, 582−588.
35. Kirby, G. W., and Robins, D. J. (1980) *Biosynthesis of Mycotoxins*, Academic Press, New York.
36. Herscheid, J. D. M., Nivard, R. J. F., Tijhuis, M. W., and Ottenheijm, H. C. J. (1980) Biosynthesis of gliotoxin. Synthesis of sulfur-bridged dioxopiperazines from N-hydroxyamino acids. *J. Org. Chem. 45*, 1885−1888.
37. Schmidt, U., Hausler, J., Ohler, E., and Poisel, H. (1979) Dehydroamino Acids, α-Hydroxy-α-amino Acids and α-Mercapto-α-amino Acids. *Fortschr. Chem. Org. Naturst. 37*, 251−327.
38. Iwasaki, T., Horikawa, H., Matsumoto, K., and Miyoshi, M. (1979) Synthetic Electroorganic Chemistry. 8. Electrochemical Synthesis and Reactivity of Alpha-Alkoxy Alpha-Amino-Acid Derivatives. *Bull. Chem. Soc. Jpn. 52*, 826−830.
39. Back, T. G., Baron, D. L., and Yang, K. (1993) Desulfurization with nickel and cobalt boride: scope, selectivity, stereochemistry, and deuterium-labeling studies. *J. Org. Chem. 58*, 2407−2413.
40. Donnelly, D. M. X., Fitzpatrick, B. M., Oreilly, B. A., and Finet, J. P. (1993) Aryllead Mediated Synthesis of Isoflavanone and Isoflavone Derivatives. *Tetrahedron 49*, 7967−7976.
41. Yan, L. Z., and Dawson, P. E. (2001) Synthesis of peptides and proteins without cysteine residues by native chemical ligation combined with desulfurization. *J. Am. Chem. Soc. 123*, 526−533.
42. Khurana, J. M., and Gogia, A. (1997) Synthetically useful reactions with nickel boride. *Org. Prep. Proc. Int. 29*, 1−32.
43. Wilson, K. A., Kalkum, M., Ottesen, J., Yuzenkova, J., Chait, B. T., Landick, R., Muir, T., Severinov, K., and Darst, S. A. (2003) Structure of Microcin J25, a Peptide Inhibitor of Bacterial RNA

Polymerase, is a Lassoed Tail. *J. Am. Chem. Soc. 125*, 12475−12483.
44. Smith, L., Zachariah, C., Thirumoorthy, R., Rocca, J., Novak, J., Hillman, J. D., and Edison, A. S. (2003) Structure and dynamics of the lantibiotic mutacin 1140. *Biochemistry 42*, 10372−10384.
45. Uteng, M., Hauge, H. H., Markwick, P. R., Fimland, G., Mantzilas, D., Nissen-Meyer, J., and Muhle-Goll, C. (2003) Three-dimensional structure in lipid micelles of the pediocin-like antimicrobial peptide sakacin P and a sakacin P variant that is structurally stabilized by an inserted C-terminal disulfide bridge. *Biochemistry 42*, 11417−11426.
46. Wang, Y., Henz, M. E., Gallagher, N. L., Chai, S., Gibbs, A. C., Yan, L. Z., Stiles, M. E., Wishart, D. S., and Vederas, J. C. (1999) Solution structure of carnobacteriocin B2 and implications for structure−activity relationships among type IIa bacteriocins from lactic acid bacteria. *Biochemistry 38*, 15438−15447.
47. Yan, L. Z., Gibbs, A. C., Stiles, M. E., Wishart, D. S., and Vederas, J. C. (2000) Analogues of bacteriocins: antimicrobial specificity and interactions of leucocin A with its enantiomer, carnobacteriocin B2, and truncated derivatives. *J. Med. Chem. 43*, 4579−4581.
48. Zheng, G., Hehn, R., and Zuber, P. (2000) Mutational analysis of the sbo-alb locus of *Bacillus subtilis*: identification of genes required for subtilosin production and immunity. *J. Bacteriol. 182*, 3266−3273.
49. Solomon, P. S., Shaw, A. L., Lane, I., Hanson, G. R., Palmer, T., and McEwan, A. G. (1999) Characterization of a molybdenum cofactor biosynthetic gene cluster in *Rhodobacter capsulatus* which is specific for the biogenesis of dimethyl sulfoxide reductase. *Microbiology 145*, 1421−1429.
50. Menendez, C., Siebert, D., and Brandsch, R. (1996) MoaA of *Arthrobacter nicotinovorans* pAO1 involved in Mo-pterin cofactor synthesis is an Fe−S protein. *FEBS Lett. 391*, 101−103.
51. Frey, P. A., and Magnusson, O. T. (2003) S-Adenosylmethionine: A wolf in sheep's clothing, or a rich man's adenosylcobalamin? *Chem. Rev. 103*, 2129−2148.
52. Clary, D. O., Wahleithner, J. A., and Wolstenholme, D. R. (1984) Sequence and arrangement of the genes for cytochrome b, URF1, URF4L, URF4, URF5, URF6 and five tRNAs in *Drosophila* mitochondrial DNA. *Nucleic Acids Res. 12*, 3747−3762.
53. Paces, V., Rosenberg, L. E., Fenton, W. A., and Kalousek, F. (1993) The beta subunit of the mitochondrial processing peptidase from rat liver: cloning and sequencing of a cDNA and comparison with a proposed family of metallopeptidases. *Proc. Natl. Acad. Sci. U.S.A. 90*, 5355−5358.
54. Braun, H. P., and Schmitz, U. K. (1995) Are the 'core' proteins of the mitochondrial bc1 complex evolutionary relics of a processing protease? *Trends Biochem. Sci. 20*, 171−175.

BI0359527